IOPscience iopscience.iop.org

Home Search Collections Journals About Contact us My IOPscience

Accurate abundance determinations in S stars

This article has been downloaded from IOPscience. Please scroll down to see the full text article.

2011 J. Phys.: Conf. Ser. 328 012014

(http://iopscience.iop.org/1742-6596/328/1/012014)

View the table of contents for this issue, or go to the journal homepage for more

Download details:
IP Address: 164.15.125.59
The article was downloaded on 01/10/2012 at 11:03

Please note that terms and conditions apply.

Journal of Physics: Conference Series **328** (2011) 012014 doi:10.1088/1742-6596/328/1/012014

Accurate abundance determinations in S stars

P Neyskens[1], S Van Eck[1], B Plez[2], S Goriely[1], L Siess[1] and A Jorissen[1]

[1]Institut d'Astronomie et d'Astrophysique, Université Libre de Bruxelles,CP 226, Boulevard du Triomphe, B-1050 Bruxelles, Belgium
[2]LUPM, Université Montpellier-II, CNRS-UMR 5024,Place Eugène Bataillon, F-34095 Montpellier, France

E-mail: pieter.neyskens@ulb.ac.be

Abstract. S-type stars are thought to be the first objects, during their evolution on the asymptotic giant branch (AGB), to experience s-process nucleosynthesis and third dredge-ups, and therefore to exhibit s-process signatures in their atmospheres. Until present, the modeling of these processes is subject to large uncertainties. Precise abundance determinations in S stars are of extreme importance for constraining e.g., the depth and the formation of the ^{13}C pocket. In this paper a large grid of MARCS model atmospheres for S stars is used to derive precise abundances of key s-process elements and iron. A first estimation of the atmospheric parameters is obtained using a set of well-chosen photometric and spectroscopic indices for selecting the *best model atmosphere* of each S star. Abundances are derived from spectral line synthesis, using the selected model atmosphere. Special interest is paid to technetium, an element without stable isotopes. Its detection in stars is considered as the best possible signature that the star effectively populates the thermally-pulsing AGB (TP-AGB) phase of evolution. The derived Tc/Zr abundances are compared, as a function of the derived [Zr/Fe] overabundances, with AGB stellar model predictions. The computed [Zr/Fe] overabundances are in good agreement with the AGB stellar evolution model predictions, while the Tc/Zr abundances are slightly over-predicted. This discrepancy can help to set stronger constraints on nucleosynthesis and mixing mechanisms in AGB stars.

1. Introduction: S stars as transition objects

The last nuclear burning stage for stars with an initial mass between ~ 0.8 M$_\odot$ and 8 M$_\odot$ occurs during the asymptotic giant branch (AGB) phase. AGB stars are known to be evolved, cool ($T_{\rm eff} < 4000$ K) and luminous (luminosity $\sim 10^4$ L$_\odot$) giant stars. The rather complex interior of AGB stars is the site of rich nucleosynthesis and mixing processes. The synthesized elements, mainly neutron-rich s-process elements and carbon, are transported to the stellar surface by the so-called third dredge-up (3DUP). The repeated occurrence of thermal pulses and 3DUPs leads to considerable changes in the chemical composition of the stellar atmosphere during its evolution on the AGB. Therefore, AGB stars can be classified into three main groups: M, S, and C stars [1]. Spectra of oxygen-rich M stars are characterized by strong TiO absorption bands, while spectra of carbon-rich C stars are dominated by C_2, CN, and CH absorption bands. Stars showing absorption bands of ZrO (in addition to TiO absorption bands) are classified as S. S stars have a carbon-over-oxygen (C/O) ratio between those of M (~ 0.5) and C stars (> 1) [2], hence they serve as interesting study objects to constrain the mixing and nucleosynthesis processes in AGB stars.

Published under licence by IOP Publishing Ltd

2. Deriving abundances of S stars

Nucleosynthesis calculations in AGB stars still suffer from many uncertainties. For example, neutrons for the s-process can be released by two reactions: ^{13}C(α,n)^{16}O and ^{22}Ne(α,n)^{25}Mg. The former reaction is activated at temperatures around 10^8 K, while the later at larger temperatures around 3×10^8 K. Details about the dominant s-process neutron source are still lacking, however observations and models hint at ^{13}C(α,n)^{16}O being the dominant neutron source in low-mass TP-AGB stars (≤ 3 M$_\odot$) [3, 4, 5]. ^{22}Ne is the dominant neutron source in more massive TP-AGB stars since the temperature during the thermal pulses is sufficiently large to activate ^{22}Ne(α,n)^{25}Mg [6]. Clues about the dominant neutron source can be obtained by deriving abundances of s-process elements (e.g., Rb, Sr) in S stars. Since ^{22}Ne produces a larger neutron flux density than ^{13}C, branching points at ^{85}Kr and ^{86}Rb can be passed to produce Rb. However, the large Rb/Zr ratios derived in massive (6–7 M$_\odot$) Large Magellanic Cloud AGB stars [7] indicate, if real, severe problems for the s-process in massive AGB stars. Even if ^{22}Ne is the dominant neutron source, it is not possible to synthesize these large amounts of Rb without also overproducing Zr. In addition, it may demonstrate the currently incomplete understanding of the analysis of the atmospheres of massive AGB stars.

The efficiency of the ^{13}C neutron source depends on the amount of protons mixed down from the H-rich envelope into the ^{12}C-rich layers. The mixed-down protons are captured by ^{12}C nuclei to trigger the chain ^{12}C(p,γ)^{13}N(β^+)^{13}C. Large uncertainties exist on the depth and the formation the ^{13}C pocket. Different extra mixing mechanisms have been proposed: convective overshooting, rotation, gravity waves, and thermohaline mixing [8, 9, 10, 11]. Although these mixing models are able to reproduce qualitatively the observed global distribution of s-elements, they are not able to reproduce quantitatively the observed overabundance of s-elements and ^{12}C.

Special attention is paid to Tc (Z=43), an element without stable isotopes. ^{99}Tc, the only isotope produced by the s-process in AGB stars, has a half-life of 2.1 $\times 10^5$ years. It is of the order of the time spent by low- and intermediate-mass stars on the TP-AGB. The increasing surface enrichment of Tc is reduced by its radioactive decay and gives rise to an almost time-independent predicted surface abundance of Tc during the ascent of the TP-AGB, while the predicted abundances of all other s-elements increase progressively [4, 12].

Consequently, it is of utmost importance to derive precise abundances of key s-elements in S stars. However, it is a difficult task because of the influence of non-solar C/O ratios on the atmospheric thermal structure [13] and due to strong TiO and ZrO molecular blending that prevent the use of equivalent widths.

Constraints on the efficiency of the 3DUP could also be set by fitting carbon-star luminosity functions (CSLF) with predictions of synthetic AGB models, using a constant free parameter for the efficiency of the 3DUP. However, it is beyond the scope of this paper.

In this paper we present derived Tc/Zr abundances, as a function of derived [Zr/Fe] overabundances, for seven intrinsic (Tc-rich) S stars belonging to the Henize sample of S stars [14]. The results are compared to the predictions of the stellar evolution code STAREVOL [15].

Constraining the initial mass of our stars is a hard task. When available, abundances of Rb and Sr can be used because temperatures that activate the ^{22}Ne neutron source are only reached in more massive AGB stars. However, mass determinations of extrinsic (Tc-poor) S stars are easier since these stars must be members of a binary star system. From an inspection of the orbital parameters of extrinsic S stars, [16] found an average mass of 1.6 M$_\odot$ with the assumption that the star's companion is a white dwarf of 0.6 M$_\odot$. However, extrinsic S stars are not populating the TP-AGB.

3. Observations

Seven Tc-rich S stars were selected from the sample of 205 Henize S stars. The sample contains both *intrinsic* and *extrinsic* S stars with R ≤ 10.5 and $\delta \leq -25°$. Optical low-resolution Boller &

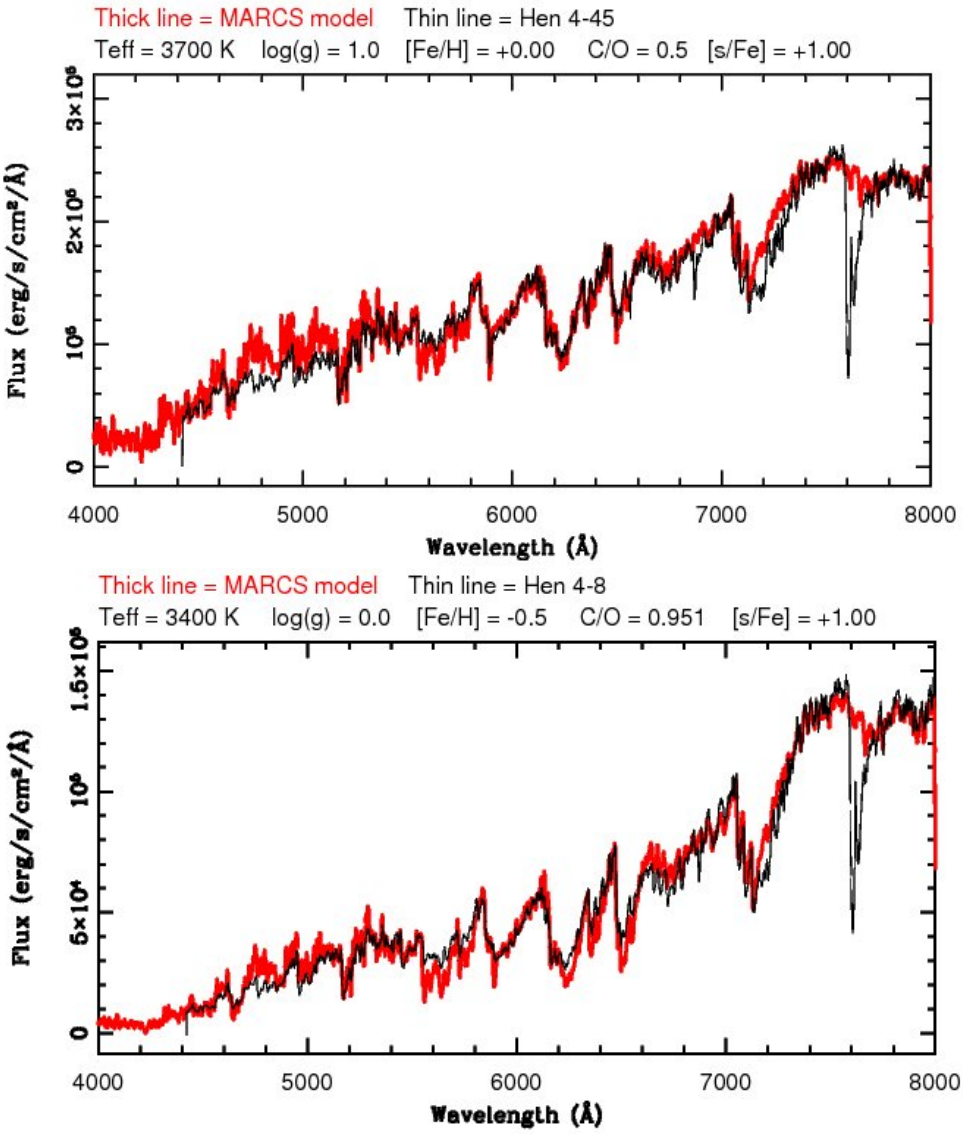

Figure 1. A comparison between the observed low-resolution optical spectrum (thin drawn black line) and the selected synthetic spectrum (boldly drawn red line) for Hen 4-45 (top panel) and Hen 4-8 (bottom panel). The atmospheric parameters of the synthetic spectra are listed in the top labels of each panel. The 7600 Å feature is from telluric O_2.

Chivens spectra ($\Delta\lambda$ =3 Å, 4400 Å – 8200 Å) were observed with the 1.52 m ESO telescope for a large fraction of the Henize S stars. High-resolution Coudé Echelle spectra ($\Delta\lambda \approx 0.08$ Å, 4220 Å – 4280 Å) were also observed with the 1.4 m CAT telescope at ESO. The presence or absence of Tc could be checked in a consistent way since the high-resolution spectra are covering two Tc I lines: Tc I 4238.191 Å and Tc I 4262.270 Å. Optical Geneva photometry and infrared SAAO $JHKL$ photometry (Catchpole, personal comm.) are also available [18, 19]. The photometric and spectroscopic data are dereddened using [20] and [21].

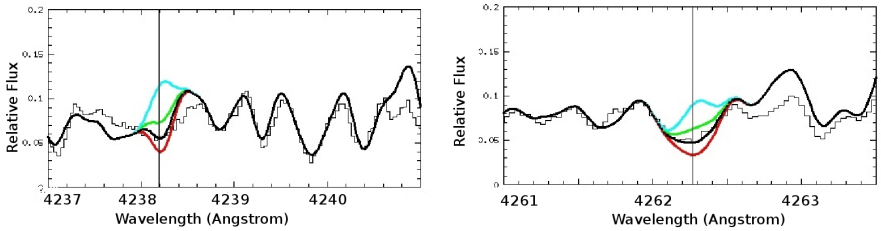

Figure 2. Tc I 4238.191 Å (left-hand panel) and Tc I 4262.270 Å (right-hand panel) for four different Tc abundances (without Tc, log ε(Tc) = 0.0, log ε(Tc) = 0.3 and log ε(Tc) = 0.6) compared to the high-resolution observation (thin drawn line) of Hen 4-162.

4. The grid of S-star MARCS atmosphere models

Dedicated model atmospheres for S stars were computed with the latest version of the MARCS code for late-type stars [22]. The constructed grid contains 3522 models and covers the following parameter space:

- 2700 K $\leq T_{\rm eff} \leq$ 4000 K (with steps of 100 K)
- 0.0 $\leq \log g \leq$ 5.0 (with steps of 1.0)
- [Fe/H] = 0.0 and -0.5
- C/O = 0.501, 0.751, 0.899, 0.925, 0.951, 0.971, and 0.991
- [s/Fe] = 0., 1., 2.
- M = 1 $M_{\odot}$
- [α/Fe] = $-0.4 \times$ [Fe/H]

The one-dimensional S-star model atmospheres are computed for different assumptions such as homogeneous stationary layers, hydrostatic and local thermodynamic equilibrium, and energy conservation by radiative and convective fluxes. Opacity sampling is applied and different continuous and line opacities are taken into account. Synthetic S stars spectra were computed using the radiative transfer code TURBOSPECTRUM [23].

5. Selecting the best atmosphere model

A first estimation of the atmospheric parameters is based on a χ^2-minimization between observed and synthetic colors (UBV & $JHKL$), and between observed with synthetic band/line-strength indices (TiO, ZrO, Na), using a so-called *best-model-finding tool*. As demonstrated by [13], the effective temperature, the C/O ratio, and the s-process enrichment are disentangled by comparing (1) observed $(V-K)_0$, $(J-K)_0$ colors with synthetic ones, and (2) observed TiO and ZrO indices with synthetic ones. Figure 1 shows the agreement, for two different S stars, between the observed low-resolution Boller & Chivens spectrum and the synthetic spectrum derived from the selected *best model atmosphere*. The agreement between the selected synthetic spectra and observed spectra is in most cases very good. However, it is sometimes difficult to choose one out of first few 'best-fit' synthetic spectra. Therefore, the error of the atmospheric parameters is computed from the range covering the first five best-fit models (i.e., the five models with the lowest χ^2 in the atmospheric parameter space). The errors are typically 100 K for $T_{\rm eff}$, 0.2 (for C/O $<$ 0.9) or 0.02 (for C/O $>$ 0.9) for C/O, and 0.5 dex for [s/Fe]. Additional uncertainties (stellar variability, errors on reddening) are inevitably still present and reliably estimating them is delicate.

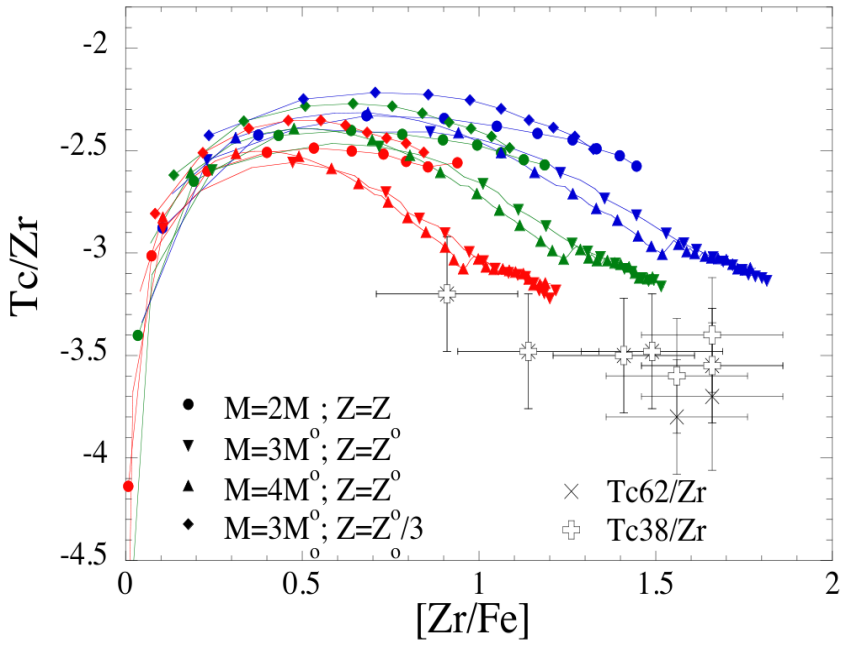

Figure 3. Comparison between observed and predicted Tc/Zr ratios as a function of the [Zr/Fe] overabundances. Four model stars with different masses and metallicities are considered (M = 2, 3, 4 $M_\odot$ at solar metallicity and M = 3 $M_\odot$ for $Z=Z_\odot/3$). For each star, the envelope s-process enrichment is calculated all along the AGB phase (the symbols correspond to the abundance ratio immediately after a 3DUP event) assuming 3 different values for the extent of the partial mixing zone λ_{pm}: for each (M,Z) model (i.e., given symbols), the leftmost curve corresponds to λ_{pm}=0.05, the rightmost to λ_{pm}=0.20, and the middle one to λ_{pm}=0.10. Observations are shown with two cross symbol types. Tc62 and Tc38 concern the Tc abundances derived from the Tc I 4262.270 Å and Tc I 4238.191 Å lines, respectively.

6. Deriving abundances of intrinsic S stars

Synthetic high-resolution spectra, based on the models computed with the derived atmospheric parameters, are next compared to high-resolution observed spectra. It allows us to fine-tune the individual chemical abundances for obtaining a good match between the observed and synthetic spectra. This way abundances of Tc, Zr, and Fe were computed. The agreement between an observed spectrum with two Tc I lines, at 4238.191 Å and 4262.270 Å, respectively, and four synthetic spectra with different Tc abundances is shown in Fig. 2.

7. Results and discussion: observed abundances vs. model predictions

Figure 3 shows the calculated Tc/Zr abundances as a function of the [Zr/Fe] overabundances. The observations are compared with s-process calculations performed on 4 AGB models computed with the stellar evolution code STAREVOL [15]. The s-process model we consider parametrizes the partial mixing of protons into the ^{12}C-rich region at the time of a 3DUP, as described in detail in [4]. The λ_{pm} parameter corresponds to the ratio of the mass of the partial mixing zone and the mass of the thermal pulse at its maximum extension. It is varied between 5% and 20% of the extent of the thermal pulse. Each symbol traces the abundance

ratio immediately after a 3DUP event.

The s-process enrichment in the stellar envelope reaches values compatible with the observations, i.e., about 1 to 2 dex enrichment for [Zr/Fe]. As is shown in Fig. 3, the Tc/Zr ratio is systematically over-predicted. Different explanations for the discrepancy can be given, in particular an increased partial decay of Tc, either during longer inter-pulse phases (e.g., in lower-mass stars), or during hotter thermal pulses.

Another problem concerns the C/O ratio. As is shown in Fig. 12 of [4], the models are already carbon-rich after four or five 3DUPs. However, the strength of the observed TiO and ZrO absorption bands of the 7 target stars clearly indicates a C/O ratio below unity. It would imply, as shown in Fig. 3, that the maximum observed [Zr/Fe] abundance has to be around 0.2 for a M=2M$_\odot$ model of solar metallicity, which is clearly not the case. This disagreement between the observed and predicted C and s-process abundances is well-known (see [4]); S stars however, with intermediate C/O ratio, allow us to investigate it with greater accuracy.

8. Perspectives

The present data will be supplemented with new data and further analyzed in a forthcoming paper. New observations, obtained with the high-resolution HERMES spectrograph [24] mounted on the Mercator telescope (La Palma), can provide additional constraints on the s-process in AGB stars. These spectra are covering a large wavelength region in the red part of the optical domain (between 7000 Å and 9000 Å) where molecular blending is less dominant than in the blue part. Abundances of C, O, and s-elements will be derived. The derivation of S stars atmospheric parameters and individual abundances, and the comparison with stellar evolution AGB models, will be performed for a larger sample of S stars.

Acknowledgments

P.N. is *Boursier F.R.I.A.*, Belgium. S.V.E., S.G. and L.S. are F.R.S.-F.N.R.S. research associates. This research has been supported by the *Communité Française de Belgique - Actions de Recherche Concertées.*

References

[1] Keenan P C 1954 *ApJ* **120** 484
[2] Iben I Jr and Renzini A 1983 *ARA&A* **21** 271
[3] Smith V V and Lambert D L 1986 *ApJ* **311** 843
[4] Goriely S and Mowlavi N 2000 *A&A* **362** 599
[5] Goriely S and Siess L 2004 *A&A* **421** 25
[6] Masseron T, Johnson J A, Plez B, Van Eck S, Primas F, Goriely S and Jorissen A 2010, *A&A* **509** 93
[7] García-Hernández D A, Manchado A, Lambert D L, Plez B, García-Lario P, D'Antona F, Lugaro M, Karakas A I and van Raai M 2009 *ApJ* **705** L31
[8] Freytag B, Ludwig H and Steffen M 1996 *A&A* **313** 497
[9] Denissenkov P A and Tout C A 2003 *MNRAS* **340** 722
[10] Siess L, Goriely S and Langer N 2004 *A&A* **415** 1089
[11] Eggleton P P, Dearborn D S P and Lattanzio J C 2006 *Science* **314** 1580
[12] Van Eck S, Jorissen A, Goriely S and Plez B 2001 *Nucl. Phys. A* **688** 45
[13] Van Eck S, Neyskens P, Plez B, Jorissen A, Edvardsson B, Eriksson K, Gustafsson B, Jørgensen U G and Nordlund Å 2011 *Proc. Why Galaxies Care About AGB STARS II: Shining Examples And Common Inhabitants (Vienna)* **445** (San Francisco : Sheridan books) p 71
[14] Henize K G 1960 *AJ* **65** 491
[15] Siess L 2007 *A&A* **476** 893
[16] Jorissen A, Van Eck S, Mayor M and Udry S 1998 *A&A* **332** 877
[17] Van Eck S, Jorissen A, Udry S, Mayor M and Pernier B 1998 *A&A* **329** 971
[18] Van Eck S and Jorissen A 1999 *A&A* **345** 127
– 2000 *A&A* **360** 196
[19] Van Eck S, Jorissen A, Udry S, Mayor M, Burki G, Burnet M and Catchpole R 2000 *A&A* **145** 51

[20] Cardelli J A, Clayton G C and Mathis J S 1989 *ApJ* **345** 245
[21] Drimmel R, Cabrera-Lavers A and López-Corredoira M 2003 *A&A* **409** 205
[22] Gustafsson B, Edvardsson B, Eriksson K, Jørgensen U G, Nordlund Å and Plez B 2008 *A&A* **486** 951
[23] Alvarez R and Plez B 1998 *A&A* **330** 1109
[24] Raskin G, Van Winckel H, Hensberge H, Jorissen A, Lehmann H, Waelkens C, Avila G, de Cuyper J P, Degroote P, Dubosson R, *et al* 2011 *A&A* **526** A69